EXECUTIVE SUMMARY OF THE THESIS

# The prognostic value of V-index in cardiovascular mortality in heart failure patients

LAUREA MAGISTRALE IN BIOMEDICAL ENGINEERING - INGEGNERIA BIOMEDICA

**Author:** LUCA DI PALMA

**Advisor:** PROF. VALENTINA CORINO

**Co-advisor:** PROF. JOSE FELIX RODRIGUEZ MATAS, DR. MASSIMO WALTER RIVOLTA

**Academic year:** 2021-2022

## 1. Introduction

Heart failure (HF) is estimated to affect one to two percent of the total adult population in industrialized nations and it continues to be a leading cause of mortality globally. Even while the treatment for acute cardiovascular disease has advanced, attempts to prevent the inevitable deterioration are often unsuccessful [1]. The primary goal of this study is to determine whether the $\mathcal{V}$-index, a new metric that has recently been proposed as an ECG marker quantifying spatial heterogeneity of ventricular repolarization, can have a predictive value for cardiovascular mortality in HF patients, alone and when adjusted for clinical covariates such as age, left ventricular ejection fraction and serum creatinine level.

## 2. Material and Methods

### 2.1. Population

The present study has analyzed a population of 380 HF patients, being part of a Holter sub-study of the GISSI-HF (Gruppo Italiano per lo Studio della Sopravvivenza nell'Infarto miocardico), who completed a 24-hour digital Holter recording at the time of enrollment. Men and women who were 18 years of age or older and had clinical evidence of HF from any cause were eligible patients. After a follow-up of $43.1 \pm 13.2$ months, 55 patients died of CV causes, mainly associated with worsening HF or sudden cardiac death.

### 2.2. Noise detection

To robustly compute the $\mathcal{V}$-index, it needs to be assessed on clean ECG segments. For this reason, the modified complete ensemble empirical mode decomposition (CEEMD) algorithm proposed by Satija et al. [2] has been used to discard noisy segments of the Holter ECG. The modified CEEMD method is used to first break down ECG signals into a residue and a number of intrinsic mode functions (IMFs), where lower-order IMFs generally capture rapid oscillation patterns of high-frequency noises, whereas higher-order IMFs frequently capture slow oscillation modes. From the IMFs, the following are computed: the high-frequency signal $h[n]$ (obtained by summing the first tree IMFs, reported in Fig.1), the LF signal $b[n]$ (the final residue, representing the baseline wander) and the ECG signal $c[n]$ (obtained by adding remaining IMFs), which include the major components of P-wave, QRS-complex and T-wave. Then,

maximum absolute amplitude (MAA) and the number of zero-crossings (NZC) are computed.
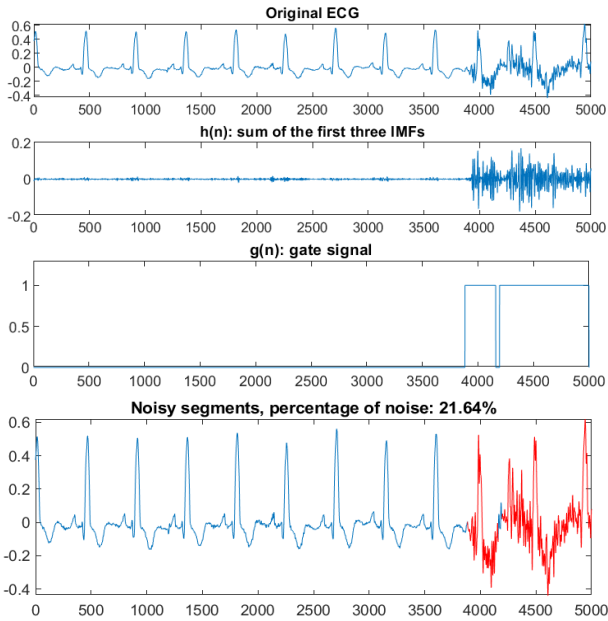


Figure 1: The original ECG segment (first row) is decomposed in its IMFs, from which $h[n]$ (second row) is computed. Then, from $h[n]$ the NZC envelope and the gate signal $g[n]$ (third row) are computed. When Equation (1) is respected, the ECG portion is labelled as noise.

If the MAA of $h[n]$ is less than a predefined threshold of $0.05mV$ the ECG signal is detected as noise-free, otherwise $h[n]$ is processed to obtain the gate signal $g[n]$, which is 1 if the NZC $> 1$, or 0 otherwise. While local pulse widths (w) corresponding to the QRS complex components generally range between 50 and 300 ms according to gate signals derived on noise-free ECG, signals corrupted with high-frequency noise appear in $g[n]$ with local pulses of extremely short duration and longer duration. For this reason, when Eq.(1) is verified, the presence of HF noise is detected.

$$HF\ Noise = \begin{cases} No, & \text{if 50 ms} < \text{w} < \text{300 ms} \\ Yes, & otherwise \end{cases} \quad (1)$$

To obtain similar results to the ones obtained in [2], in the current study the same ECG window of $10s$ has been considered, such as the same thresholds.

## 2.3.   $\mathcal{V}$-index

The electrophysiological model of the surface ECG put forward by van Oosterom [3] and a statistical model of the myocytes' repolarization timings [4, 5] are combined to create the $\mathcal{V}$-index. Van Oosterom demonstrated how a weighted sum of the myocytes' transmembrane potentials can be used to model the structure of the T-wave on the surface ECG in a single beat. A weighted sum of a single function $T_d(t)$ (the so-called *dominant T-wave*) and its derivatives can be used to approximate the multi-lead surface ECG in a first approximation since the repolarization phase of the action potential is comparable across myocytes at a particular heart rate:

$$\Psi(t) \approx -A\Delta\rho T_d(t) + \frac{1}{2}A\Delta\rho^2 \dot{T}_d(t)$$

where $\Psi$ is the $[L \times 1]$ ECG, with $L$ being the number of leads, the terms $w_1, w_2$ are $[L \times 1]$ vectors of lead factors, $A$ is a patient-dependent $[L \times M]$ transfer matrix accounting for the contribution of each node to the $L$-leads electrocardiographic recording in $\Psi(t)$ and $\Delta\rho = [\Delta\rho_1(k), \Delta\rho_2(k), ..., \Delta\rho_M(k)]^T$ is a vector of repolarization delays. Sassi and Mainardi [4] proposed a model for the repolarization delay $\Delta\rho_m$ for each cell $m$, obtained by dividing the myocardium in $M$ cells, as follows:

$$\Delta\rho_m(k) = \rho_m(k) - \overline{\rho(k)} = \theta_m + \varphi_m(k)$$

where $\overline{\rho(k)}$ is the average repolarization time in the single beat $k$ over the set of $M$ cells; $\theta_m$ models the spatial variability of the repolarization times for a given subject at a given heart rate; $\varphi_m(k)$ describes differences in repolarization times which are observable among successive beats (the temporal variability of the repolarization times). An estimate $\mathcal{V}_i$, where $i$ represents the $i_{th}$ lead, of the standard deviation of $\theta_m$ is given by

$$\mathcal{V}_i = \frac{std[w_2(i)]}{std[w_1(i)]} \approx \left(\sum_{m=1}^{M} \frac{\theta_m^2}{M}\right)^{1/2} = s_\theta$$

After scanning the entire 24h ECG recordings with the CEEEMD algorithm in leads I, II and V2, 10-minute segments composed of at least 20% of clean 10-second segments (in all three leads) were selected for the $\mathcal{V}$-index computation.

## 2.4. Cox proportional-hazards model

The method used in this study for modelling the connection between variables and survival or other censored outcome is the Cox proportional hazards model [6]. Considering $X_i$ as the vector of covariate for the $i_{th}$ person, the hazard for the individual $i$ is specified by the Cox model as follows:

$$\lambda_i(t) = \lambda_0(t)e^{X_i\beta}$$

where $\lambda_0$ represents the baseline hazard, an undefined nonnegative function of time, and $\beta$ is a $p \times 1$ vector of coefficients. The model specifies how the baseline hazard of patient $i$ changes with the variables $X_i$.

The hazard ratio for two subjects with fixed covariate vectors $X_i$ and $X_j$, computed as:

$$\frac{\lambda_i(t)}{\lambda_j(t)} = \frac{\lambda_0(t)e^{X_i\beta}}{\lambda_0(t)e^{X_j\beta}} = \frac{e^{X_i\beta}}{e^{X_j\beta}}$$

is constant over time, and for this reason, the model is also known as the proportional hazards model. Starting from the partial likelihood (PL) function introduced by Cox [6], it's possible to estimate the set of coefficients $\beta$. Computing and differentiating the log PL with respect to $\beta$, the score vector $U(\beta)$ is obtained. At this point, the maximum PL estimator is found by solving $U(\hat{\beta}) = 0$.

## 2.5. Cosinor Analysis

In order to investigate if the $\mathcal{V}$-index follows a cyclic rhythm, a further investigation using the cosinor model [7] has been conducted. The cosinor model, which is a technique for modelling cyclical variation, fits a cosine curve to data using the Least Squares process. It is possible to write the regression model for a single-component cosinor as:

$$y(t) = M + A\cos\left(\frac{2\pi t}{\tau} + \phi\right) + e(t)$$

where $M$ is the mesor, $A$ is the amplitude, $\phi$ is the acrophase (a measure of the time of peak reoccurring in each cycle), $e(t)$ is the error term and $\tau$ is the period, which has been imposed to be of 24 hours. Minimizing the residual sum of squares , the normal equations are obtained and used to estimate $M$, $A$ and $\phi$. The null hypothesis $H_0$ (no rhythm is present) is rejected when $F > F_{1-\alpha}(2, N-3)$, where $N$ is the number of samples, $\alpha$ the specified probability threshold and $F$ the result of the $F$-test.

## 3. Results

### 3.1. Population

Clinical variables of alive and CV dead patients were compared using the t-test or Wilcoxon test for numerical variables and $\chi^2$ for categorical variables. CV dead patients were older ($p < 0.0001$), with higher values in creatinine ($p < 0.0001$), and smaller values in LVEF ($p < 0.01$). Also, they have a higher incidence of NSVT ($p < 0.0001$) a more advanced NYHA class ($p = 0.02$) and had less BBL treatment ($p < 0.01$), while no significant difference is related to the gender of the patients ($p = 0.78$).

### 3.2. Noise Detection

The number of clean 10-minute segments was 65 $\pm$ 38, 63 $\pm$ 38, and 66$\pm$ 38 for visit 2, visit 4, and visit 6 respectively, with no significant differences between the number of segments computed on alive or CV dead patients (Wilcoxon test, $p = 0.86$, $p = 0.08$, $p = 0.18$)

### 3.3. $\mathcal{V}$-index

In the first visit, the number of patients for which the $\mathcal{V}$-index was computed in at least one segment is 365 patients out of the 380 available recordings. At time visit 4, out of the 375 alive patients, 326 underwent the ECG recording and 307 had at least one $\mathcal{V}$-index value. In visit 6, the number of patients with available $\mathcal{V}$-index value decreased to 301 out of the 320 who underwent the ECG recording (out of the 360 patients that were still alive). The cosine function has been fitted for each patient with at least 5 available $\mathcal{V}$-index values for each visit. An example of the behaviour of the $\mathcal{V}$-index during the day, along with cosinor fittings, is illustrated in Figure 2. The $F$-test shows that 72%, 69% and 70% of the patients in visits 2, 4, and 6 respectively follow a circadian rhythm.

The mesor for alive and CV dead patients was found to be different in visit 2 only (p<0.05), whereas no significant differences were found in the amplitude for any of the three visits.

In addition to mesor and amplitude, $\mathcal{V}$-index mean, median, standard deviation (std) and $\mathcal{V}$-index on the first available segment (FS), have
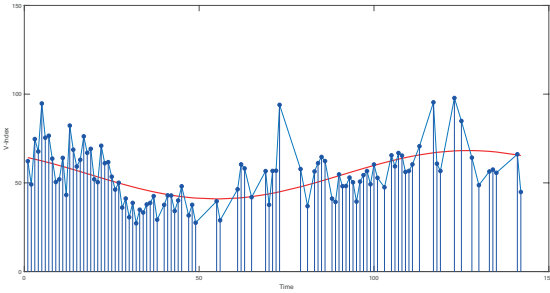
Figure 2: On the X-axis, the 24 hours are divided into 144 10-minute segments. Each blue dot represents a $\mathcal{V}$-index value. The red line is the estimated cosine function.

been considered to summarize $\mathcal{V}$-index values for each patient. For $\mathcal{V}$-index mean, median and $\mathcal{V}$-index computed on the FS statistically significant differences have been found in visit 2 between alive and CV dead patients ($p < 0.05$). In addition to the statistics previously mentioned, a new signature has been computed starting from coefficients of a bivariate Cox model using mesor (M, 0.55) and amplitude (A, 0.22):

$$Signature = 0.55 \cdot M + 0.22 \cdot A$$

Distributions of the $\mathcal{V}$-index signature for CV dead and alive patients in visit 2 are statistically different ($p = 0.04$) according to the single tail Wilcoxon test, while no differences are present for visit 4 and visit 6 ($p = 0.08, 0.15$).

In order to dichotomize numerical variables, thresholds (reported in Table 1) were found by computing the receiver operating characteristic (ROC) curve and selecting the value associated with the best FPR,TPR combination.

| Variable | Threshold |
|---|---|
| $\mathcal{V}$-index mean, v2 | 33.24 ms |
| $\mathcal{V}$-index median, v2 | 40.35 ms |
| $\mathcal{V}$-index std, v2 | 11.54 ms |
| $\mathcal{V}$-index mesor, v2 | 26.6 ms |
| $\mathcal{V}$-index amplitude, v2 | 6.64 ms |
| $\mathcal{V}$-index signature, v2 | 15.25 ms |
| $\mathcal{V}$-index first segment, v2 | 32.81 ms |
| Creatinine | 1.2 mg/dL |

Table 1: The selected thresholds for each variable that has been binarized. v: visit

## 3.4.  Survival analysis

A first step has been made by using Kaplan-Meier (K-M) method to assess if the variable alone can separate the starting population into two groups with different survival probabilities. Considering visit 2, significant differences between the two groups (obtained by splitting the population according to the selected threshold) have been found (nonparametric log-rank test) in $\mathcal{V}$-index mean ($p = 0.01$), $\mathcal{V}$-index median ($p < 0.01$), $\mathcal{V}$-index signature ($p = 0.01$), $\mathcal{V}$-index mesor ($p = 0.02$) and $\mathcal{V}$-index on the FS ($p < 0.01$). In the other visits, only the $\mathcal{V}$-index computed on the FS preserves its significance ($p < 0.01$ in visit 4 and $p = 0.02$ in visit 6), reported in Figure 3. Then, a univariate (reported in Table 2) and multivariate (reported in Table 3) (adjusted for age) Cox model has been computed for each variable. When selecting the best multivariate Cox model, for comparison reasons, the same clinical variables in [8] were considered as candidate predictors: age $\geq 70$ years, sex, ischaemic cardiomyopathy, (New York Heart Association) NYHA class III–IV, left ventricular ejection fraction (LVEF), heart rate, systolic arterial pressure, presence of non-sustained ventricular tachycardia (NSVT), the number of premature ventricular contractions/h, creatinine, sodium, and presence of beta-blocker (BBL) treatment. In order to prevent overfitting the maximum number of candidate clinical predictors, to combine with one of the $\mathcal{V}$-index metrics, was chosen equal to 4, such that the rule of having maximum z/10 variables is respected, being z the numbers of events (55 CV death events in this case).

| | HR (95% CI) | p-value | C-index |
|---|---|---|---|
| $\mathcal{V}$-index mean | 1.91 (1.10-3.32) | 0.02 | 0.57 |
| $\mathcal{V}$-index median | 2.23 (1.28-3.87) | <0.005 | 0.58 |
| $\mathcal{V}$-index mesor | 2.29 (1.11-4.72) | 0.02 | 0.57 |
| $\mathcal{V}$-index amplitude | 1.48 (0.84-2.60) | 0.17 | 0.55 |
| $\mathcal{V}$-index signature | 2.64 (1.18-5.87) | 0.02 | 0.58 |
| $\mathcal{V}$-index std | 1.69 (0.99-2.90) | 0.06 | 0.56 |
| $\mathcal{V}$-index FS | 2.40 (1.39-4.15) | <0.005 | 0.59 |

Table 2: Results of the univariate Cox models, applied at the time of visit 2

The best model selection (evaluating C-index) computed at the time of visit 2 is composed of age $\geq 70$ years [HR: 3.06 95% CI (1.69-5.54),
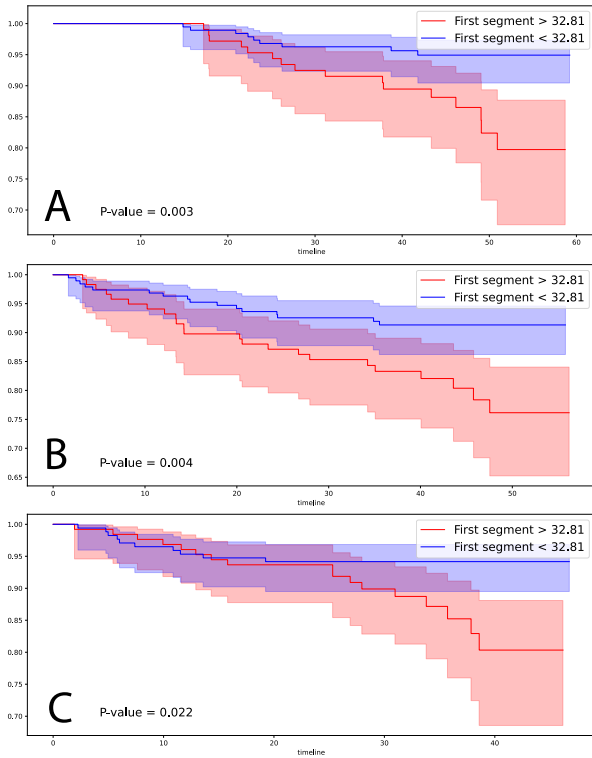
Figure 3: K-M curves of the $\mathcal{V}$-index computed on the FS. A: visit 2, B: visit 4, C: visit 6

$p < 0.005$], creatinine $\geq 1.2$ mg/dL [HR: 2.78 95% CI (1.54-5.02), $p < 0.005$], presence of NSVT [HR: 2.12 95% CI (1.18-3.82), $p < 0.005$], LVEF [HR: 0.96 95% CI (0.93-0.99), $p = 0.02$] and signature $\geq 15.25$ ms [HR: 2.56 95% CI (1.14-5.72), $p = 0.02$], obtaining a C-index of 0.78. This represents an improvement with respect to a C-index of 0.76 obtained by the best-performing clinical model, composed of age, creatinine, NSVT and LVEF.

The same experiments were repeated in visit 4 and visit 6. The only variable which has preserved its relevance in all three visits, using the same threshold found in visit 2, is the $\mathcal{V}$-index on the FS. The univariate Cox [HR: 2.46 95% CI (1.30-4.65), $p = 0.01$] applied at visit 4, such as the multivariate model adjusted for age (HR: 2.26 95% CI (1.19-4.28), $p = 0.01$) confirms that patients with $\mathcal{V}$-index on the FS $> 32.81$ ms are associated with a doubled risk of death with respect to patients with a $\mathcal{V}$-index on the FS $< 32.81$ ms. The best multivariate model that has been found in visit 4 is composed of age $\geq 70$ years [HR: 3.04 95% CI (1.54-6.03), $p < 0.005$], NSVT presence [HR: 2.02 95% CI (1.04-3.92), $p = 0.04$], BBL treatment [HR: 0.44 95% CI (0.23-0.85), $p = 0.01$], LVEF [HR: 0.96

| | HR (95% CI) | p-value | C-index |
|---|---|---|---|
| $\mathcal{V}$-index mean | 1.76 (1.02-3.06) | 0.04 | 0.68 |
| $\mathcal{V}$-index median | 2.03 (1.17-3.53) | 0.01 | 0.68 |
| $\mathcal{V}$-index mesor | 2.05 (0.99-4.23) | 0.05 | 0.69 |
| $\mathcal{V}$-index amplitude | 1.43 (0.82-2.52) | 0.21 | 0.69 |
| $\mathcal{V}$-index signature | 2.40 (1.08-5.34) | 0.03 | 0.69 |
| $\mathcal{V}$-index std | 1.59 (0.93-2.72) | 0.09 | 0.67 |
| $\mathcal{V}$-index FS | 2.26 (1.31-3.91) | <0.005 | 0.69 |

Table 3: Each row represents a multivariate Cox model, composed of the written statistic adjusted for age, at time visit 2.

95% CI (0.92-1.00), $p = 0.06$], $\mathcal{V}$-index on the FS $\geq 32.81$ ms [HR: 2.19 95% CI (1.15-4.18), $p = 0.02$], obtaining a C-index of 0.78. Considering visit 6, in the univariate model the $\mathcal{V}$-index on the FS is still significant [HR: 2.42 95% CI (1.11-5.30), $p = 0.03$], while not when adjusted for age [HR: 2.13 95% CI (0.97-4.67), $p = 0.06$]. The best model obtained at time visit 6 when combining $\mathcal{V}$-index with other clinical variables is composed of age $\geq 70$ years [HR: 3.04 95% CI (1.30-7.12), $p = 0.01$], creatinine $\geq 1.2$ mg/dL [HR: 3.15 95% CI (1.36-7.28), $p = 0.01$], BBL treatment [HR: 0.54 95% CI (0.25-1.18), $p = 0.12$], NSVT presence [HR: 1.94 95% CI (0.87-4.33), $p = 0.10$] and $\mathcal{V}$-index on the FS $\geq 32.81$ ms [HR: 1.8 95% CI (0.84-4.12), $p = 0.13$], obtaining a C-index of 0.81.

## 4.   Conclusions

This study shows the potential of using the $\mathcal{V}$-index as a predictor of cardiovascular mortality in heart failure patients. The use of $\mathcal{V}$-index statistics combined with clinical variables (age, serum creatinine, the incidence of NSVT, LVEF, NYHA class and BBL treatment) increase performances in risk stratification in HF patients. Greater values of $\mathcal{V}$-index are associated with a higher risk of death in HF patients, as confirmed in previous study [9, 10] for different conditioned patients. Considering the $\mathcal{V}$-index statistics analyzed in this study, the median value of the 24h ECG recording appears to be a more robust and reliable parameter with respect to the mean to summarize the $\mathcal{V}$-index behaviour in a day. The application of the cosinor analysis to derive mesor and amplitude, and consequently the $\mathcal{V}$-index signature, provides additional information about the daily behaviour of the $\mathcal{V}$-index. Also

considering the $\mathcal{V}$-index computed only on the first segment, the $\mathcal{V}$-index preserves its significance and its prognostic value.

Threshold values found in visit 2 identify at higher risk patients with $\mathcal{V}$-index mean and median value greater than 33.24 ms and 40.35 ms, respectively. Also, values of the $\mathcal{V}$-index signature greater than 15.25 ms are associated with a higher risk of CV death, such as values of the $\mathcal{V}$-index on the first segment greater than 32.81 ms. However, the use of the same thresholds found in visit 2 applied in visit 4 and visit 6 appears to be non-optimal. This can be due to the smaller populations present at the time of visit 4 and visit 6. Indeed, while available observations of $\mathcal{V}$-index in visit 2 were 365, this number has decreased to 307 (-16%) in visit 4 and to 301 in visit 6 (-18%).

Comparing the $\mathcal{V}$-index performance with autonomic markers computed in [8] on slightly the same population, the results obtained in this study exploit the relevance of $\mathcal{V}$-index in predicting cardiovascular mortality. The best results obtained in this study in visit 2, resulting from multivariate Cox models achieved by combining a clinical model with, respectively, the $\mathcal{V}$-index signature (C-index=0.78), the $\mathcal{V}$-index mesor (C-index=0.78) and $\mathcal{V}$-index median (C-index=0.76), are in line with results obtained in [8] with standard deviation of all normal-to-normal RR intervals (0.76), the power in the very LF bands (0.79), the power in the LF bands (0.79), the short-term fractal scaling exponent measured by the detrended fluctuation analysis (0.76) and turbulence slope (0.75).

In conclusion, this study shows that the use of $\mathcal{V}$-index has a relevant prognostic value in HF patients and its use should be further investigated.

## References

[1] S. Dassanayaka and S. P. Jones, "Recent developments in heart failure," *Circulation Research*, vol. 117, sep 2015.

[2] U. Satija, B. Ramkumar, and M. S. Manikandan, "Automated ECG noise detection and classification system for unsupervised healthcare monitoring," *IEEE Journal of Biomedical and Health Informatics*, vol. 22, pp. 722–732, may 2018.

[3] A. van Oosterom, "ECGSIM: an interactive tool for studying the genesis of QRST waveforms," *Br. Heart J.*, vol. 90, pp. 165–168, Feb. 2004.

[4] R. Sassi and L. T. Mainardi, "An estimate of the dispersion of repolarization times based on a biophysical model of the ECG," *IEEE Transactions on Biomedical Engineering*, vol. 58, pp. 3396–3405, dec 2011.

[5] R. Sassi, L. T. Mainardi, P. Laguna, and J. F. Rodriguez, "Validation of the -index through finite element 2d simulations," in *Computing in Cardiology 2013*, vol. 40, pp. 337–340, 2013.

[6] D. R. Cox, "Regression models and life-tables," *Journal of the Royal Statistical Society: Series B (Methodological)*, vol. 34, no. 2, pp. 187–202, 1972.

[7] G. Cornelissen, "Cosinor-based rhythmometry," *Theoretical Biology and Medical Modelling*, vol. 11, apr 2014.

[8] M. T. L. Rovere, G. D. Pinna, R. Maestri, S. Barlera, M. Bernardinangeli, M. Veniani, G. L. Nicolosi, R. Marchioli, and L. T. and, "Autonomic markers and cardiovascular and arrhythmic events in heart failure patients: still a place in prognostication? data from the GISSI-HF trial," *European Journal of Heart Failure*, vol. 14, pp. 1410–1419, dec 2012.

[9] M. W. Rivolta, L. T. Mainardi, R. C. Reis, M. O. C. Rocha, A. L. P. Ribeiro, F. Lombardi, and R. Sassi, "Spatial repolarization heterogeneity and survival in chagas disease," *Methods of Information in Medicine*, vol. 53, no. 06, pp. 464–468, 2014.

[10] M. W. Rivolta, L. T. Mainardi, R. Laureanti, R. Sassi, M. Kühne, N. Rodondi, G. Conte, G. Moschovitis, V. Schlageter, S. Aeschbacher, D. Conen, T. Reichlin, L. Roten, S. Osswald, C. S. Zuern, A. Auricchio, and V. D. Corino, "Association between ventricular repolarization parameters and cardiovascular death in patients of the SWISS-AF cohort," *International Journal of Cardiology*, vol. 356, pp. 53–59, jun 2022.